HHS Public Access

Author manuscript

Acc Chem Res. Author manuscript; available in PMC 2019 September 18.

Published in final edited form as:

Acc Chem Res. 2018 September 18; 51(9): 2047–2063. doi:10.1021/acs.accounts.8b00233.

Hierarchical Assemblies of Supramolecular Coordination Complexes

Sougata Datta[*], **Manik Lal Saha**[*], and **Peter J. Stang**[*]

Department of Chemistry, University of Utah, 315 South 1400 East, Room 2020, Salt Lake City, Utah 84112, United States

CONSPECTUS:

Hierarchical self-assembly (HAS) is a multilevel organization process that first assembles elementary molecular units into ordered secondary structures via noncovalent interactions, which further act as the building blocks to form more complex multifunctional superstructures at the next level(s). The HAS strategy has been used as a versatile method for the preparation of soft-matter nanoarchitectures of defined size and morphologies, tunable luminescence, and biological importance. However, such preparation can be greatly simplified if well-defined dynamic structures are employed as the cores that upon linking form the desired nanoarchitectures. Discrete supramolecular coordination complexes (SCCs) with well-defined shapes, sizes, and internal cavities have been widely employed to construct hierarchical systems with functional diversity. This Account summarizes the prevailing strategies used in recent years in the preparation of SCC-based HASs and illustrates how the combination of dynamic metal–ligand coordination with other interactions was used to obtain hierarchical systems with interesting properties.

HASs with dual orthogonal interactions involving coordination-driven self-assembly and hydrogen bonding/host–guest interaction generally result in robust and flexible supramolecular gels. Likewise, hybridization of SCCs with a suitable dynamic covalent network via a hierarchical strategy is useful to prepare materials with self-healing properties. The intrinsic positive charges of the SCCs also make them suitable precursors for the construction of HASs via electrostatic interactions with negatively charged biological/abiological molecules. Furthermore, the interplay between the hydrophilic and lipophilic characters of HASs by varying the number and spacial orientation of alkyl/oxyethylene chains of the SCC is a simple yet controllable approach to prepare ordered and tunable nanostructures. Certain SCC-cored hierarchical systems exhibit reversible polymorphism, typically between micellar, nanofiber, and vesicular phases, in response to various external perturbations: heat, photoirradiation, pH-variance, redox-active agents, etc. At the same time, multiple noncovalent interaction mediated HASs are growing in numbers and are promising candidates for obtaining functionally diverse materials.

The photophysical properties of SCC-based HASs have been used in many analytical applications. For example, embedding tetraphenylethene (TPE)-based pyridyl ligands within metallo-supramolecular structures partially restricts the molecular rotations of its phenyl rings, endowing

[*]**Corresponding Authors** sougata.datta@utah.edu. [*] manik.saha@utah.edu. [*] stang@chem.utah.edu.

Notes

The authors declare no competing financial interest.

the resultant SCCs with weak emissions. Further aggregation of such HASs in suitable solvents results in a marked enhancement in emission intensity along with quantum yields. They act as sensitive sensors for different analytes, including pathogens, drugs, etc. HASs are also useful to develop multidrug systems with cooperative chemotherapeutic effects. Hence, the use of HASs with theranostic SCCs combining cell-imaging agents and chemotherapeutic scaffolds is a promising drug delivery strategy for cancer theranostics. At the same time, their responsiveness to stimuli, oftentimes due to the dynamic nature of the metal–ligand interactions, play an important role in drug release via a disassembly mechanism.

Graphical Abstract

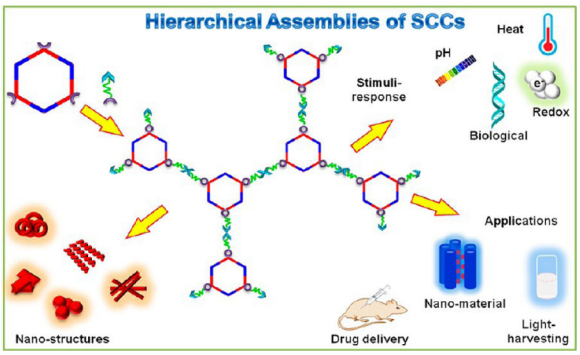

1. INTRODUCTION

Hierarchical self-assembly (HAS) via multiple noninterfering interactions is the basis of forming various complex biological superstructures, such as double-stranded DNA, three-dimensionally folded proteins, and biologically active cell membranes, that are important for life. For example, in hemoglobin, multiple noncovalent interactions including metal coordination, hydrogen-bonding, hydrophobic interactions, electrostatic interactions, etc. contribute to its structure and properties, where the heme groups, that is, the porphyrin–metal complexes, are responsible for the transportation of O_2 in the metabolic process. Inspired by Nature, chemists have been increasingly investigating such intricate pathways in synthetic supramolecular systems within abiological (nonbiological) self-assembly. This burgeoning field has seen rapid growth in the last decades, providing a new class of functional nanomaterials capable of adjusting their order in response to damage or stimulus.

Likewise, coordination-driven self-assembly has evolved into a viable methodology for constructing well-defined, discrete supramolecular coordination complexes (SCCs), ranging from two-dimensional (2-D) polygons to three-dimensional (3-D) cages, prisms, and polyhedra.[1–6] Compared to the classical covalent approach, the metal–ligand coordination strategy offers considerable synthetic advantages such as few steps, as well as fast and facile preparation of the defect-free final products.[7] The orthogonality of metal-ligand coordination with other noncovalent interactions leads to some novel hierarchical designs, wherein coordination-driven self-assembly can be used to construct a metallacyclic core; while the final hierarchical constructs are obtained via use of a second different interaction (Figure 1). The orientation and the number of the complementary functional groups in the

building blocks of the HAS play an important role in determining the morphology, properties, and functionality of the resultant architecture. Metal–ligand interactions with moderate bond energies (ca. 15–25 kcal/mol) endow them with well-defined core geometry, which provides precise control over the numbers, locations, and relative orientations of the functional groups in the hierarchical construct.[8–10] The dynamic character of metal–ligand interactions also allows them to undergo reversible switching of structure, morphology, and function in response to various external stimuli, such as pH, temperature, or stress, which then further provides a flexible and robust platform for developing adaptive and functional materials.[11,12]

This Account describes the recent development of metallacycle- or cage-based HASs wherein metal–ligand interactions constitute the core and other orthogonal interactions, such as hydrogen bonding, π–π stacking, host–guest complexation, electrostatic and hydrophobic or hydrophilic interactions, and dynamic covalent bonding, have been employed to obtain a second or third level of hierarchy in the system. Specifically, we describe SCC-based hierarchical organizations depending on the number and types of noncovalent interactions and provide useful insights into how their combination with metal–ligand coordination helps in evolving their unique properties. The use of HASs based on SCCs in the area of nanomaterials, light harvesting, sensing, drug delivery, etc. is also discussed.

2. HIERARCHICAL SELF-ASSEMBLIES CONSTRUCTED VIA DUAL ORTHOGONAL INTERACTIONS

2.1. Metal–Ligand Coordination and Hydrogen-Bonding

Self-complementary molecular components with multiple hydrogen-bonding units can form stable aggregates depending upon the experimental conditions. Meijer and Sijbesma have developed a novel, self-complementary quadruple hydrogen-bonding motif, 2-ureido-4-pyrimidinone (UPy) ($\Delta G \approx 10$ kcal mol^{-1}, $K_{dim} > 10^7$ M^{-1} in chloroform) that has been widely employed in constructing supramolecular polymers.[13] The unification of UPy motifs and various metal–ligand interactions in a single process have also provided hierarchical architectures of different topologies.

For instance, the coordination driven self-assembly of a 120° dipyridyl ligand **1** and organoplatinum(II)-acceptors **2, 3**, or **4**, resulted in rhomboid **8** and hexagons **9** and **10**, respectively, having free UPy groups at the alternate vertices (Chart 1).[14] Subsequently, linear chain (for the rhomboid) or cross-linked (for the hexagons) supramolecular polymers, respectively, were obtained via linking the metallacycles though the hydrogen-bonding of the UPy-units in CH_2Cl_2 (Figure 2). Upon swelling in organic solvents, the cross-linked polymer formed viscoelastic gels, which further led to macroscopic fibers of sufficient robustness to form stable knots.[14]

Using a similar protocol, metallacyclic cored dendritic supramolecular polymers (DSPs) were prepared by Yan et al. (Figure 3A).[15] Concentration- and temperature-dependent diffusion-ordered NMR spectroscopy (DOSY) data suggest that the monomer concentration as well as temperature had significant effects on these polymerization processes.

Dynamic light scattering (DLS) indicated that the sizes of these polymers are dependent on the degree-of-branching of the dendrons attached to the metallacyclic core. DSP **13** with its most branched dendrons formed nanofibers having molecular width of calculated ~ 5.88 nm, observed ~ 6.00 nm (Figure 3B,C). The steric hindrance exerted by the bulky dendrons at the vertices of the rhomboids likely acted as the driving force for the linear-chain supramolecular polymerization and is responsible for the formation nanofibers of such high aspect ratio. However, small nanoparticles with diameters of ~6.00 nm were observed in DMSO presumably because of the disruption of intermolecular hydrogen-bonding by the polar solvent (Figure 3D). Hence, a combination of metal–ligand coordination and hydrogen-bonding is suitable for the preparation of a HAS in nonpolar solvents.

2.2. Metal–Ligand Coordination and π–π Stacking

By combining π–π stacking and metal–ligand interactions, Yang and co-workers recently demonstrated the HAS of a metallacycle **16**[16] and a metallacage **17**[17] functionalized with alkynylplatinum(II) 2,6-bis(benzimidazol-2′-yl)pyridine (bzimpy) moieties (Figure 4A–C). These SCCs formed yellow metallogels (critical gelator concentration (CGC) = 7.2 and 7.5 mg mL^{-1} for 16 (Figure 4B) and17 (Figure 4C), respectively) at room temperature without the aid of a conventional heating–cooling method. The gelation process was driven by intermolecular Pt···Pt and π–π stacking interactions of the peripheral alkynylplatinum(II) bzimpy units. The addition of 1 equiv of coronene to the metallogel obtained from **16** triggered a gel-to-sol transition due to the disruption of the aforesaid intermolecular interactions (Figure 4B). The presence of excess (10 equiv) pyrene, anthracene, 1-naphthol, tetraphenylethylene, and carbazole, the gel remains stable, demonstrating that this stimuli-responsive gel can be used in the visual recognition of coronene.

2.3. Metal–Ligand Coordination and Host–Guest Interactions

In contrast to hydrogen bonding interactions and π–π stacking, host–guest interactions provide better directional and non-self-complementary properties. Hence, hierarchical self-assembly involving metal–ligand coordination and host–guest interaction is an efficient approach to build complex architectures. The choice of solvent is also important for the preparation of these HASs. For example, crown ether- and pillararene-based HASs mainly form in organic solvents, such as chloroform, acetone, and acetonitrile, while an aqueous medium is more suitable for the cyclodextrin- and cucurbituril-based HASs.

Huang's group utilized a [2]pseudorotaxane host–guest complexation between the benzo-21-crown-7 (B21C7) moiety of a hexagonal organoplatinum(II) metallacycle **18** and a bisammonium salt **19** to form a cross-linked supramolecular polymer network (SPN) that transformed into a thermoreversible gel in a CH_2Cl_2/CH_3CN mixture at concentrations higher than 20 mM (Figure 5).[18] The reversible gel-to-sol transition was achieved via the addition and removal of KPF_6, wherein the K^+ ions deconstruct the B21C7/ammonium linkages to form a more stable B21C7/K^+ complex, resulting in the decomposition of the gel. The gelation can be restored by masking the K^+ ions with a better ligand, such as dibenzo-18- crown-6. Likewise, Lu et al. recently reported that a multifunctional metallacage-cored supramolecular gel formed by orthogonal metal-coordination and host–guest interactions.[19]

Li et al. also prepared cross-linked supramolecular polymers via HAS, involving metal–ligand coordination and pillar[5]-arene-based host–guest recognition.[20] Organoplatinum(II) hexagons of different sizes containing pillar[5]arene hosts alternatively at the vertices were employed to prepare host–guest supramolecular polymers using a neutral ditopic dinitrile guest as cross-linking agent. These supramolecular polymers transformed into stable metallogels at higher concentrations. The dynamic nature of Pt–N bonds and host–guest interactions allowed these gels to undergo reversible gel–sol transitions upon application of different stimuli, such as temperature, halides, and competitive guests, due to the disassembly and reassembly of the polymer networks.

Figure 6 shows a pillar[5]arene-based dipyridyl donor **20**, which formed different supramolecular polymers upon mixing with di-Pt(II) or tri-Pt(II) acceptors (**21** or **22**).[21] Further cross-linking of these polymers with a neutral ditopic dinitrile guest **23** led to two 3D SPNs, which subsequently resulted in two multi-stimuli-responsive metallogels. These metallogels exhibited significant differences in their rheological behaviors attributed to the different hierarchical organizations in the gels. These types of novel cavity-containing metallogels may have potential applications in the areas of catalysis, absorption, separation, etc.

2.4. Metal–Ligand Coordination and Electrostatic Interactions

Electrostatic interactions are far less directional and specific than host–guest interactions. The high density of ionic charges in the self-assembly leads to materials with significant stability and mechanical strength. At the same time, the strong ionic interactions decrease the opportunities for relaxation and rearrangements, which is a major disadvantage for macroscopic alignment. Electrostatic interaction mediated self-assembly of simple precursors to complex supramolecules has been extensively employed in the construction of molecular capsules, monolayers, helical nanoribbons, etc., as well as in determining the structure, dynamics, and function of biomolecules (e.g., protein folding, pH-induced conformational changes, and molecular recognition).[22,23] Since, the majority of SCCs are highly charged because of the presence of oxidized metal species as electron acceptors, they can act as an ideal platform for the construction of hierarchical architectures via electrostatic interactions, but this strategy is limited to ionic precursors and mainly applicable in polar solvents.

DNA condensation is a process of compacting DNA molecules and has many potential applications in medicinal chemistry and biotechnology.[24] Fujita's group utilized a peptide-coated $Pd_{12}L_{24}$ nanosphere **24** to mimic histone, a natural DNA-compacting protein (Figure 7A).[25] The comparable surface charge density (+1.2 nm^{-2}) and diameter (8.4 nm with fully extended peptide chains) of **24** to the histone octamer facilitate a compound **24**-triggered stepwise DNA condensation (Figure 7B). At a concentration of 42 nM, binding of **24** with cyclic plasmid pBR322 DNA (total charge ratio (Z_{24}/Z_{DNA}) = 0.87; Z_{24} and Z_{DNA} denote the total positive and negative charges derived from sphere **24** and the DNA molecules in the mixture, respectively) led to a "beads-on-a-string" like structure (form I) as observed with atomic force microscopy (AFM) (Figure 7C). When the concentration of **24** was increased to 83 nM (Z_{24}/Z_{DNA} = 1.7), larger aggregates consisting of DNA and nanoparticles associated

with the “multistrand aggregation” form (form II) were observed. A further increment in the concentration of **24** to 0.42 mM (Z_{24}/Z_{DNA} = 8.7), resulted in a structural transition of the DNA into a compact globule form (form III) (Figure 7D). These results indicate that DNA condensation occurred via a HAS mechanism similar to the natural nucleosome assembly.

2.5. Metal–Ligand Coordination and Dynamic Covalent Bonding

Since dynamic covalent bonds (DCBs) combine the reversible character of noncovalent interactions with the robustness of covalent bonds, they have been employed extensively to prepare adaptive materials with mechanical stability and interesting properties such as self-healing, stimuli-responsiveness, etc.[26,27] Recently, Fujita, Kato, and co-workers have reported a self-healing liquid crystalline (LC) gel obtained via the combination of coordination driven self-assembly and dynamic covalent bonding.[28] As shown in Figure 8, the spherical coordination complex **26** ($Pd_{12}L_{24}$), containing **24** mesogenic fork-like dendrons connected via flexible tri-(ethylene glycol) spacers, exhibited lyotropic LC behavior (smectic phases) in DMF. Hybridization of this complex with a dynamic covalent network formed via the reaction between the aldehyde groups of **27** and the hydrazide moieties of **28** in a DMF–DMSO mixture resulted in a free-standing LC gel with self-healing properties. The self-healing property of the gel was attributed to the dynamic character of the acylhydrazone linkages, and the LC assembly was retained even in the gel phase as confirmed by small-angle X-ray diffraction study. This example shows how a hierarchical combination of coordination driven self-assembly and dynamic covalent bonding is useful to obtain self-healing materials without compromising the mechanical strength.

2.6. Metal–Ligand Coordination and Hydrophobic Interactions

Zhang et al. recently reported the HAS of a series of discrete metallacycles having pendent long alkyl chains that formed various nanostructures via hydrophobic interactions.[29] The rhomboid **29** formed a nanofibrous network in CH_2Cl_2/ CH_3OH (1:1) under *n*-hexane diffusion after 84 h, whereas the hexagons **30** and **31** exhibited nanospheres under the same conditions (Figure 9). Furthermore, a change in the solvent polarity also modulated the morphology of the rhomboid from a nanofiber (CH_2Cl_2/CH_3OH, 1:1) to a nanosphere (CH_2Cl_2/ CH_3OH, 7:1). Various morphologies of the metallacycles were attributed to the differences in the population and spatial orientation of the hydrophobic chains around the metallacyclic cores. Hence, this sheds light on the HAS phenomenon, where precise morphological (shape and size) control of the nanostructures of the SCCs could be obtained by fine-tuning of their hydrophilic/lipophilic characters.

Likewise, Stang’s group prepared two amphiphilic rhomboids that exhibited concentration dependent morphologies.[30] Rhomboids **35** and **36** self-assembled into spherical micellar structures with diameters of 50–100 and 70–150 nm, respectively, at a low concentration (5.00×10^{-6} M), while they transformed into 1D nanofibers (10–50 nm) and 2D nanoribbons, respectively, at a 10-fold higher concentration (Figure 10A,B). Moreover, viscoelastic metallohydrogels were obtained at critical gelator concentrations of 4.56 wt % for **35** and 5.55 wt % for **36**. This provides a useful strategy to prepare different HASs by modulating the self-organization of a single molecule (SCC-to-micelle-to-hydrogel).

Although many examples of organogels using SCC motifs are known, SCC-based hydrogels are still rare.

Recently, a series of alanine-based chiral metallacycles, rhomboids **37**$^{\mathbf{D}}$ and **37**$^{\mathbf{L}}$ and hexagons **38**$^{\mathbf{D}}$ and **38**$^{\mathbf{L}}$, were prepared for the fabrication of chiral nanostructures (Figure 10A,C).[31] Similar to the previous report, the metallacycles exhibited nanospheres at a low concentration in methanol, while metallogels were obtained at a high concentration driven by hydrophobic interactions. The molecular chirality of the alanine-based metallacycles transformed into supramolecular chirality upon gelation, as they formed helical nanofibers in the gel phase as confirmed by electron microscopy. This was further supported by the intense CD bands of the gels in the range of 230–400 nm. However, no characteristic CD signature was observed in the sol suggesting the crucial role of gelation in the molecular chirality transfer to the microscopic level.

3. HIERARCHICAL SELF-ASSEMBLIES DERIVED BY MULTIPLE ORTHOGONAL INTERACTIONS

Zhou et al. reported an efficient strategy to prepare supramolecular polymers by combining triple orthogonal noncovalent interactions, metal–ligand coordination, hydrogen bonding, and host–guest interactions, in a single process.[32] A hexagonal metallacycle **41** decorated with UPy and B21C7 groups at the periphery was prepared via the organoplatinum←pyridyl coordination-driven self-assembly (Figure 11). The self-complementary hydrogen-bonding between the UPy groups led to a hexagonal cavity cored supramolecular polymer network, wherein the B21C7 groups remain available for additional postfunctionalization. This network formed self-healing gels at high concentrations or upon solvent swelling. Moreover, emissive components, such as perylene or tetraphenylethylene, were introduced into the network via crown ether–dialkylammonium salt based host–guest interactions, providing light-emitting polymers.

While traditional supramolecular polymers are prepared from a single monomeric unit, supramolecular copolymers (SCs) are comprised of two different monomers and thereby may provide additional functional properties. Figure 12 shows an orthogonal strategy to prepare a rhomboidal metallacycle cored linear SC by combining multiple noncovalent interactions.[33] The UPy-functionalized mechanically interlocked subunit **43** and rhomboid **44** were prepared by crown-ether-based [2]rotaxane host–guest interactions and the Pt(II) ←pyridyl directional bonding approaches, respectively. Both **43** and **44** independently formed linear supramolecular polymers via self-complementary hydrogen-bonding of the UPy units; their 1:1 mixture in CH_2Cl_2 led to a linear SC randomly linked by mechanically interlocked moieties and hydrogen-bonded metallacycles. The thermal stability and diffusion coefficient of the resulting SC were approximately the average of the linear supramolecular polymers of **43** and **44**.

An emissive metallogel via HAS was prepared by Xu and coworkers using a hexagonal metallacycle decorated with tetraphenylethylene (TPE), amide groups, and hydrophobic long alkyl chains at the periphery.[34] While the solution of the metallacycle exhibited weak emission, strong green fluorescence emission was observed in the gel phase at the same

concentration, attributed to the aggregation induced emission (AIE) of the TPE units. Addition of tetrabutylammonium bromide (TBAB) transformed the gel to a yellow turbid solution due to destruction of the hexagonal metallacycle via dissociation of the Pt–N bonds. The gel phase could be restored by removal of the Br^- using $AgPF_6$. The importance of the hydrogen-bonding interactions of the amide groups in the gelation process was demonstrated by deprotonation of the −N-H protons using tetrabutylammonium fluoride, which triggered a gel-to-sol transition, while reprotonation using $HClO_4$ recovered the gel phase again suggesting the reversibility of the gel-to-sol transition process.

[2]Catenane Pd_nL_{2n} ($n = 8$) metallo-supramolecular architectures **45–47** composed of two interlocked D_{4h}-symmetric Pd_4L_8 barrel-shaped containers were recently reported by Clever and co-workers (Figure 13A).[35] The cavities of such large “Hopf link” catenane structures were occupied by the NO_3^- counterions, which played a crucial role in the interpenetration of the Pd_4L_8 barrel-shaped monomers as confirmed by ESI-MS and X-ray crystallographic analysis. This was further supported by structural transformation of a mixture of $Pd_3L'_6$ (**48**) and $Pd_4L'_8$ (**49** and **50**) assemblies in the presence of NO_3^- anions to the interpenetrated structure 45 (Figure 13B). The structural rearrangement of the mixture of **48–50** did not occur upon extended heating (70 °C, 24 h) or in the presence of PF_6^- anions, indicating the importance of NO_3^- in this process. Furthermore, the hexyloxy-functionalized catenane **47** hierarchically self-assembled into vesicle-like aggregates, which could be reversibly disassembled by increasing the temperature as observed by DLS and TEM experiments (Figure 13C). In contrast, **45** and **46** failed to form aggregated structures due to the shorter alkyl chains on their respective ligands

4. FUNCTIONAL ASPECTS

4.1. Light-Emitting Materials

Viruses, due to their precise nanoscaled dimensions, structural uniformity, and complexity, have been extensively used in the preparation of hybrid nanomaterials.[36] For instance, tobacco mosaic virus (TMV) possesses a unique tube-like structure with a dimension of 300 nm in length, 18 nm in outer diameter, and 4 nm in inner diameter. This virus is comprised of 2130 identical coat proteins arranged helically around a single strand of RNA and remains stable at temperatures up to 60 °C and at pH values between 2 and 10. These unique features make TMV a promising scaffold for the development of hierarchical nanostructures.

Tian et al. recently prepared well-defined 3D biohybrids via the HAS of a TPE-based discrete, organoplatinum(II) metallacycle **51** with TMV or bacteriophage (M13).[37] The nanoconfinement of the metallacycle within these biohybrids via electrostatic interactions resulted in a marked fluorescence enhancement (Figure 14), due to the further restriction of intramolecular rotation of the TPE units. Both **TMV/51** and **M13/51** biohybrids exhibited a 5.41- and 9.58-fold fluorescence enhancement over free **51**, respectively. Under UV-light, these strong emissions can be observed by the naked eye, although a solution of **51** is only weakly emissive. In addition, the individual virus could be released via dissociation of **51** using TBAB, making such HASs promising as dynamic optical or biofunctional materials.

White light emitting organic molecules have gained attention for their fundamental importance and practical applications in low energy consumption lighting devices.[38] In contrast to the single molecule white light emitter, it is relatively easier to achieve white light emission via the HAS of multicomponents with the emission color covering the entire visible range. However, poor stability and performance, less reproducibility, etc. are the issues that are often encountered during device fabrication from such mixed emitter systems.

Recently, Yin and co-workers demonstrated the concentration-dependent tunable emission of a supramolecular oligomer, derived via the host–guest interactions between the crown ether units of a rhomboidal organoplatinum(II) metallacycle **52** and a fluorescent bis-ammonium linker **53** at a 1:1 molar ratio (Figure 15).[39] At high concentrations of the precursors (>0.5 mM), the resultant hierarchical constructs exhibited an orange emission, indicating that the metallacycle based emissions are predominant, while the blue emission of the bis-ammonium linker strongly influenced the spectrum at concentrations below 25 μM. The ensemble emitted white light at a concentration of 29 μM, thus providing an efficient approach for the construction supramolecular assemblies with tunable emissive properties.

4.2. Sensing

Heparin is a naturally occurring, highly sulfated negatively charged polysaccharide derived from alternate repeating units of 1–4-linked pyranosyl uronic acid and 2-amino-2-deoxy-glucopyranose units.[40] It has been used as an anticoagulant drug in cardiopulmonary surgery and in the treatment of thrombotic diseases; however, an overdose of heparin can exert adverse effects such as hemorrhages and heparin-induced thrombocytopenia. A careful sensing and quantification of the heparin level in blood serum is crucial from a medical perspective. Chen et al. employed the AIE property of a HAS comprised of a TPE-based cationic organoplatinum(II) metallacycle **54** and heparin for the selective detection and quantification of heparin at the clinical dosage level (Figure 16).[41] The heparin triggered emission enhancement is due to the hierarchical arrangement of the positively charged metallacycle and the negatively charged linear heparin, which was further supported by a single bead chain like morphology as observed under atomic force microscopy. The unique hierarchical construct likely caused this high selectivity over other structurally similar compounds such as chondroitin 4-sulfate, hyaluronic acid, and protamine sulfate. Hence, SCC-based HAS is a potential platform for developing highly sensitive and selective sensors for bioanalyte detection. However, further modification is needed to make such sensors reusable and economically viable for practical applications.

Recently, the concepts of coordination-driven self-assembly and postassembly reversible addition–fragmentation chain-transfer polymerization have been unified in a single process to synthesize a hexagonal organoplatinum(II)–metallacycle cored supramolecular star block copolymer **25** (Figure 17).[42] The resulting polymer showed lower critical solution temperature (LCST) behavior (Tcloud = 33 °C) at a low concentration (ca. 3 mg/mL), due to the presence of poly(*N*-isopropylacrylamide) (PNIPAAM) units in the polymeric scaffold.

In addition, it also exhibited a CO_2-triggered reversible spherical micelle-to-vesicle morphological transformation, guided by its poly(*N*,*N*-dimethylaminoethyl methacrylate) (PDMAEMA) segments. The coil-like folded arrangement of the block copolymer chains

transformed to an unfolded state due to electrostatic repulsion, attributed to a carbonic acid induced protonation of the dimethylamino groups of the PDMAEMA, which caused the morphological transformation. This transformation was reversed by the removal of dissolved CO_2 with N_2. At a higher concentration (ca. 25 mg/mL), bubbling of CO_2 into the aqueous solution of **25** and subsequent heating at 34 °C, instantaneously, resulted in an injectable and cytocompatible hydrogel. The hydrogel could be reverted to the sol state by cooling to room temperature.

4.3. Encapsulation and Release

Yang's group demonstrated the HAS of a peripherally dimethyl isophthalate (DMIP) functionalized poly(benzyl ether) metallodendrimer containing a well-defined hexagonal metallacyclic core.[43] The metallodendrimer **56** formed vesicle-like nanostructures in an acetone–THF mixture (4:1) driven by π–π stacking and CH–π and hydrogen bonding interactions associated with the DMIP-functionalized poly(benzyl ether) dendrons as confirmed by various microscopy techniques (Figure 18). The obtained vesicles transformed to micelles upon addition of TBAB due to the disassembly of the hexagonal metallacyclic core via Pt–N bond dissociation. The original vesicular morphology was restored by adding $AgPF_6$ to the mixture indicating the reversibility of this transformation. Fluorescent dyes such as BODIPY and sulforhodamine B were successfully encapsulated in the vesicles. The halide responsive morphological transition feature of the vesicles was further utilized for subsequent controlled release of the encapsulated dye molecules.

HASs of ruthenium and platinum based SCCs have recently been used in biological applications, specifically as anticancer agents. However, the intrinsic hydrophobicity of the majority of such SCCs limits their biomedical applications. Grafting of an amphiphilic copolymer with the SCC backbone induces sufficient water solubility and allows loading of additional anticancer drug(s) into the polymeric scaffold via HAS to achieve a synergistic anticancer effect.

Recently Yu et al. reported a metallacycle-cored amphiphilic polymer **57** containing four diblock copolymer arms (Figure 19A).[44] These polymer arms contain glutathione (GSH)-responsive 2-azido-methylbenzoate units. In the metallacycle, the AIE-active TPE-based dipyridyl donor is employed as a fluorescent probe for live cell imaging, while the 3,6-bis[*trans*-$Pt(PEt_3)_2$]phenanthrene (**PhenPt**) acted an anticancer drug. The presence of the AIE-active TPE-motif endows **57** with a better photostability compared to the conventional fluorophores. The anticancer activity of **PhenPt** is attributed to its ability to cross-link with DNA via coordination with the purine bases (Figure 19B). This inhibits the DNA repair mechanisms, resulting in DNA damage and subsequently inducing cell apoptosis. The amphiphilic character of **57** allows it to form nanoparticles (NPs) of different sizes and vesicles, depending upon the experimental conditions. Anticancer drugs, like doxorubicin (DOX) or DOX·HCl were encapsulated in the cavities of these nanostructures (Figure 19C).

The entrapped drug was subsequently released in a controlled manner by the disassembly of the nanostructures via a GSH-stimulated cascade elimination reaction. In contrast to free DOX·HCl, a synergistic antitumor activity with low systemic toxicity was observed for ~50 nm DOX-loaded NPs, which was due to an enhanced permeability and retention effect. The

tumor inhibition rate for DOX-loaded NPs (loaded DOX = 27.4%) was 81.6% in contrast to 19.5% for free DOX· HCl, indicating a superior antitumor efficacy of the DOX-loaded NPs. Hence, synergistic combination of multiple therapeutic agents via HAS is a promising prospect in cancer therapy. Such a hierarchical strategy may be useful for the efficient delivery of poorly water-soluble anticancer drugs to cancer cells by the judicious implementation of multiple orthogonal interactions in a single process.

5. CONCLUSION

In summary, we have discussed the recent advances in the field of HAS of metallacycles and metallacages with a particular focus on their properties and functions. The orthogonality of metal–ligand coordination with other noncovalent interactions has been a key feature of these designs (Table 1), while the potential to incorporate stimuli-responsive scaffolds into the structures and the dynamic nature of the noncovalent interactions endow the systems with stimuli-responsive characters. Given these properties, many of these systems have proven to be useful as sensors, light-emitting nanomaterials, and antitumor agents.

Nonetheless, some important aspects are yet underexplored (Figure 20): (i) Water-soluble HASs of SCCs have not been well-developed, which may be applicable as new drug carriers, delivery agents, etc. (ii) There is a strong demand in the current scientific community to rationally design and prepare novel soft materials having a unique combination of robustness, adaptivity, stimuli-responsiveness, self-healing, and recyclability. In this regard, SCC-based gels are, for instance, prospective systems; however, they often suffer from poor mechanical strengths and stabilities.

The incorporation of single-walled carbon nanotubes or graphene could synergistically enhance the mechanical strengths and may endow the resultant hybrid gels with better mechanical properties.[45] (iii) From the point of view of responsiveness, sophisticated mechanochromic or -luminescent SCC-based HAS may be developed. Furthermore, responsiveness toward biological stimuli needs to be explored in order to mimic the functions and properties of biological systems. (iv) Whereas many SCC-based hierarchical architectures involving dual orthogonal interactions have been developed, future research may provide complex superstructures derived via multiple interactions. We believe that the methodologies described herein will motivate chemists to further exploit developing multifunctional, hierarchical supramolecular materials, which will enrich nanotechnology, material science, and biology.

ACKNOWLEDGMENTS

P.J.S. and S.D., respectively, thank the NIH (Grant R01-CA215157) and SERB Indo-U.S. Postdoctoral fellowship for financial support.

Biographies

Sougata Datta obtained his B.Sc. degree in chemistry from the Ramakrishna Mission Vidyamandira, Belur Math, University of Calcutta (India) in 2007. He received his M.Sc. (2009) and Ph.D. (2015) in organic chemistry from the Indian Institute of Science,

Bangalore (India), and is currently investigating the stimuli-responsive and biological properties of organoplatinum(II) based supramolecular systems as a postdoctoral fellow in the group of Peter J. Stang at the University of Utah.

Manik Lal Saha has been a postdoctoral fellow and the Cosupervisor of Professor Peter Stang's group at the University of Utah for the past 3.5 years. Prior to this, he received his B.Sc. Honours (2006), M.Sc. (2008), and Ph.D. (2014) in chemistry from the University of Calcutta (India), IIT Kanpur (India), and the University of Siegen (Germany), respectively. His research accomplishments to date have resulted in over 35 publications, and currently he is investigating the biological and materials aspects of organoplatinum(II) derived self-assemblies.

Peter J. Stang is the David P. Gardner distinguished professor of Chemistry. He is a member of the US National Academy of Sciences and a foreign member of the Chinese Academy of Sciences, the recipient of the Chinese Government "International Cooperation Award in Science and Technology" (2016), the ACS Priestley Medal (2013), and the US National Medal of Science (2011).

REFERENCES

(1). Chen L-J; Yang H-B; Shionoya M Chiral Metallosupramolecular Architectures. Chem. Soc. Rev 2017, 46, 2555–2576. [PubMed: 28452389]

(2). Cook TR; Stang PJ Recent Developments in the Preparation and Chemistry of Metallacycles and Metallacages via Coordination. Chem. Rev 2015, 115, 7001–7045. [PubMed: 25813093]

(3). Lifschitz AM; Rosen MS; McGuirk CM; Mirkin CA Allosteric Supramolecular Coordination Constructs. J. Am. Chem. Soc 2015, 137, 7252–7261. [PubMed: 26035450]

(4). Newkome GR; Moorefield CN From 1 → 3 Dendritic Designs to Fractal Supramacromolecular Constructs: Understanding the Pathway to the Sierpiński Gasket. Chem. Soc. Rev 2015, 44, 3954–3967. [PubMed: 25316287]

(5). Brown CJ; Toste FD; Bergman RG; Raymond KN Supramolecular Catalysis in Metal–Ligand Cluster Hosts. Chem. Rev 2015, 115, 3012–3035. [PubMed: 25898212]

(6). Harris K; Fujita D; Fujita M Giant Hollow M_nL_{2n} Spherical Complexes: Structure, Functionalisation and Applications. Chem. Commun 2013, 49, 6703–6712.

(7). Chakrabarty R; Mukherjee PS; Stang PJ Supramolecular Coordination: Self-Assembly of Finite Two- and Three-Dimensional Ensembles. Chem. Rev 2011, 111, 6810–6918. [PubMed: 21863792]

(8). Ko C-C; Yam VW-W Coordination Compounds with Photochromic Ligands: Ready Tunability and Visible Light-Sensitized Photochromism. Acc. Chem. Res 2018, 51, 149–159. [PubMed: 29265804]

(9). Saha ML; Yan X; Stang PJ Photophysical Properties of Organoplatinum(II) Compounds and Derived Self-Assembled Metallacycles and Metallacages: Fluorescence and its Applications. Acc. Chem. Res 2016, 49, 2527–2539. [PubMed: 27736060]

(10). McConnell AJ; Wood CS; Neelakandan PP; Nitschke JR Stimuli-Responsive Metal-Ligand Assemblies. Chem. Rev 2015, 115, 7729–7793. [PubMed: 25880789]

(11). Clever GH; Punt P Cation-Anion Arrangement Patterns in Self-Assembled Pd_2L_4 and Pd_4L_8 Coordination Cages. Acc. Chem. Res 2017, 50, 2233–2243. [PubMed: 28817257]

(12). Wang W; Wang Y-X; Yang H-B Supramolecular Transformations within Discrete Coordination-Driven Supramolecular Architectures. Chem. Soc. Rev 2016, 45, 2656–2693. [PubMed: 27009833]

(13). Beijer FH; Sijbesma RP; Kooijman H; Spek AL; Meijer EW Strong Dimerization of Ureidopyrimidones via Quadruple Hydrogen Bonding. J. Am. Chem. Soc 1998, 120, 6761–6769.

(14). Yan X; Li S; Pollock JB; Cook TR; Chen J; Zhang Y; Ji X; Yu Y; Huang F; Stang PJ Supramolecular Polymers with Tunable Topologies via Hierarchical Coordination-Driven Self-Assembly and Hydrogen Bonding Interfaces. Proc. Natl. Acad. Sci. U. S. A 2013, 110, 15585–15590. [PubMed: 24019475]

(15). Yan X; Jiang B; Cook TR; Zhang Y; Li J; Yu Y; Huang E; Yang H-B; Stang PJ Dendronized Organoplatinum(II) Metallacyclic Polymers Constructed by Hierarchical Coordination-Driven Self-Assembly and Hydrogen-Bonding Interfaces. J. Am. Chem. Soc 2013, 135, 16813–16816. [PubMed: 24187961]

(16). Jiang B; Zhang J; Zheng W; Chen L-J; Yin G-Q; Wang Y-X; Sun B; Li X; Yang H-B Construction of Alkynylplatinum-(II) Bzimpy-Functionalized Metallacycles and Their Hierarchical Self-Assembly Behavior in Solution Promoted by Pt···Pt and π-π Interactions. Chem. - Eur. J 2016, 22, 14664–14671. [PubMed: 27533298]

(17). Zhang Y; Zhou Q-F; Huo G-F; Yin G-Q; Zhao X-L; Jiang B; Tan H; Li X; Yang H-B Hierarchical Self-Assembly of an Alkynylplatinum(II) Bzimpy-Functionalized Metallacage via Pt···Pt and π-π Interactions. Inorg. Chem 2018, 57, 3516–3520. [PubMed: 29251490]

(18). Yan X; Cook TR; Pollock JB; Wei P; Zhang Y; Yu Y; Huang F; Stang PJ Responsive Supramolecular Polymer Metallogel Constructed by Orthogonal Coordination-Driven Self-Assembly and Host/Guest Interactions. J. Am. Chem. Soc 2014, 136, 4460–4463. [PubMed: 24621148]

(19). Lu C; Zhang M; Tang D; Yan X; Zhang Z; Zhou Z; Song B; Wang H; Li X; Yin S; Sepehrpour H; Stang PJ Fluorescent Metallacage-Core Supramolecular Polymer Gel Formed by Orthogonal Metal Coordination and Host-Guest Interactions. J. Am. Chem. Soc 2018, 140, 7674–7680. [PubMed: 29856215]

(20). Li Z-Y; Zhang Y; Zhang C-W; Chen L-J; Wang C; Tan H; Yu Y; Li X; Yang H-B Cross-Linked Supramolecular Polymer Gels Constructed from Discrete Multi-pillar[5]arene Metallacycles and Their Multiple Stimuli-Responsive Behavior. J. Am. Chem. Soc 2014, 136, 8577–8589. [PubMed: 24571308]

(21). Li Z; Xing H; Shi B Two novel supramolecular metallogels constructed by platinum(II) coordination and pillar [5]arene-based host-guest interactions. Polym. Chem 2017, 8, 2747–2751.

(22). Sastry M; Rao M; Ganesh KN Electrostatic Assembly of Nanoparticles and Biomacromolecules. Acc. Chem. Res 2002, 35, 847–855. [PubMed: 12379137]

(23). Zhou H-X; Pang X Electrostatic Interactions in Protein Structure, Folding, Binding, and Condensation. Chem. Rev 2018, 118, 1691–1741. [PubMed: 29319301]

(24). Bracha D; Karzbrun E; Daube SS; Bar-Ziv RH Emergent Properties of Dense DNA Phases toward Artificial Biosystems on a Surface. Acc. Chem. Res 2014, 47, 1912–1921. [PubMed: 24856257]

(25). Kikuchi T; Sato S; Fujita D; Fujita M Stepwise DNA condensation by a histone-mimic peptide-coated $M_{12}L_{24}$ spherical complex. Chem. Sci 2014, 5, 3257–3260.

(26). Li J; Nowak P; Otto S Dynamic Combinatorial Libraries: From Exploring Molecular Recognition to Systems Chemistry. J. Am. Chem. Soc 2013, 135, 9222–9239. [PubMed: 23731408]

(27). Wei Z; Yang JH; Zhou J; Xu F; Zrínyi M; Dussault PH; Osada Y; Chen YM Self-Healing Gels Based on Constitutional Dynamic Chemistry and Their Potential Applications. Chem. Soc. Rev 2014, 43, 8114–8131. [PubMed: 25144925]

(28). Uchida J; Yoshio M; Sato S; Yokoyama H; Fujita M; Kato T Self-Assembly of Giant Spherical Liquid-Crystalline Complexes and Formation of Nanostructured Dynamic Gels that Exhibit Self-Healing Properties. Angew. Chem., Int. Ed 2017, 56, 14085–14089.

(29). Zhang J; Marega R; Chen L-J; Wu N-W; Xu X-D; Muddiman DC; Bonifazi D; Yang H-B Hierarchical Self-Assembly of Supramolecular Hydrophobic Metallacycles into Ordered Nanostructures. Chem. - Asian J 2014, 9, 2928–2936. [PubMed: 25139814]

(30). Yan X; Li S; Cook TR; Ji X; Yao Y; Pollock JB; Shi Y; Yu G; Li J; Huang F; Stang PJ Hierarchical Self-Assembly: Well- Defined Supramolecular Nanostructures and Metallohydrogels via Amphiphilic Discrete Organoplatinum(II) Metallacycles. J. Am. Chem. Soc 2013, 135, 14036–14039. [PubMed: 23927740]

(31). Sun Y; Li S; Zhou Z; Saha ML; Datta S; Zhang M; Yan X; Tian D; Wang H; Wang L; Li X; Liu M; Li H; Stang PJ Alanine-Based Chiral Metallogels via Supramolecular Coordination Complex Platforms: Metallogelation Induced Chirality Transfer. J. Am. Chem. Soc 2018, 140, 3257–3263. [PubMed: 29290113]

(32). Zhou Z; Yan X; Cook TR; Saha ML; Stang PJ Engineering Functionalization in a Supramolecular Polymer: Hierarchical Self-Organization of Triply Orthogonal Non-covalent Interactions on a Supramolecular Coordination Complex Platform. J. Am. Chem. Soc 2016, 138, 806–809. [PubMed: 26761393]

(33). Wei P; Yan X; Cook TR; Ji X; Stang PJ; Huang F Supramolecular Copolymer Constructed by Hierarchical Self-Assembly of Orthogonal Host-Guest, H-Bonding, and Coordination Interactions. ACS Macro Lett 2016, 5, 671–675.

(34). Ren Y-Y; Xu Z; Li G; Huang J; Fan X; Xu L Hierarchical Self-Assembly of a Fluorescence Emission-Enhanced Organogelator and its Multiple Stimuli-Responsive Behaviors. Dalton Trans 2017, 46, 333–337. [PubMed: 27921100]

(35). Bloch WM; Holstein JJ; Dittrich B; Hiller W; Clever GH Hierarchical Assembly of an Interlocked M_8L_{16} Container. Angew. Chem., Int. Ed 2018, 57, 5534–5538.

(36). Niu Z; Liu J; Lee LA; Bruckman MA; Zhao D; Koley G; Wang Q Biological Templated Synthesis of Water-Soluble Conductive Polymeric Nanowires. Nano Lett 2007, 7, 3729–3733. [PubMed: 18020388]

(37). Tian Y; Yan X; Saha ML; Niu Z; Stang PJ Hierarchical Self-Assembly of Responsive Organoplatinum(II) Metallacycle-TMV Complexes with Turn-On Fluorescence. J. Am. Chem. Soc 2016, 138, 12033–12036. [PubMed: 27608138]

(38). Smith MD; Karunadasa HI White-Light Emission from Layered Halide Perovskites. Acc. Chem. Res 2018, 51, 619–627. [PubMed: 29461806]

(39). Zhang M; Yin S; Zhang J; Zhou Z; Saha ML; Lu C; Stang PJ Metallacycle-Cored Supramolecular Assemblies with Tunable Fluorescence Including White-Light Emission. Proc. Natl. Acad. Sci. U. S. A 2017, 114, 3044–3049. [PubMed: 28265080]

(40). Linhardt RJ; Toida T Role of Glycosaminoglycans in Cellular Communication. Acc. Chem. Res 2004, 37, 431–438. [PubMed: 15260505]

(41). Chen L-J; Ren Y-Y; Wu N-W; Sun B; Ma J-Q; Zhang L; Tan H; Liu M; Li X; Yang H-B Hierarchical Self-Assembly of Discrete Organoplatinum(II) Metallacycles with Polysaccharide via Electrostatic Interactions and Their Application for Heparin Detection. J. Am. Chem. Soc 2015, 137, 11725–11735. [PubMed: 26322626]

(42). Zheng W; Yang G; Shao N; Chen L-J; Ou B; Jiang S-T; Chen G; Yang H-B CO_2 Stimuli-Responsive, Injectable Block Copolymer Hydrogels Cross-Linked by Discrete Organoplatinum(II) Metallacycles via Stepwise Post-Assembly Polymerization. J. Am. Chem. Soc 2017, 139, 13811–13820. [PubMed: 28885839]

(43). Chen L-J; Zhao G-Z; Jiang B; Sun B; Wang M; Xu L; He J; Abliz Z; Tan H; Li X; Yang H-B Smart Stimuli-Responsive Spherical Nanostructures Constructed from Supramolecular Metallodendrimers via Hierarchical Self-Assembly. J. Am. Chem. Soc 2014, 136, 5993–6001. [PubMed: 24684256]

(44). Yu G; Zhang M; Saha ML; Mao Z; Chen J; Yao Y; Zhou Z; Liu Y; Gao C; Huang F; Chen X; Stang PJ Antitumor Activity of a Unique Polymer That Incorporates a Fluorescent Self-Assembled Metallacycle. J. Am. Chem. Soc 2017, 139, 15940–15949. [PubMed: 29019660]

45. () Cheng C; Li S; Thomas A; Kotov NA; Haag R Functional Graphene Nanomaterials Based Architectures: Biointeractions, Fabrications, and Emerging Biological Applications. Chem. Rev 2017, 117, 1826–1914. [PubMed: 28075573]

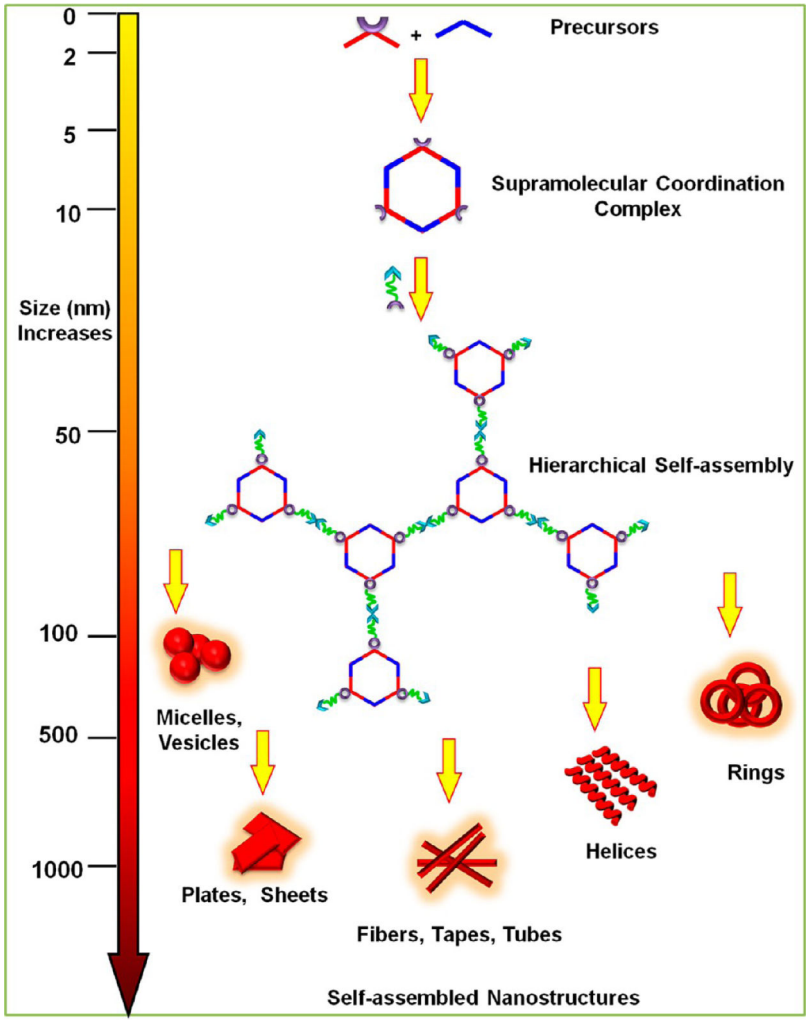

Figure 1.

Preparation of a hexagonal SCC from suitable precursors via coordination driven self-assembly and its HAS into well-defined nanostructures using multiple orthogonal interactions.

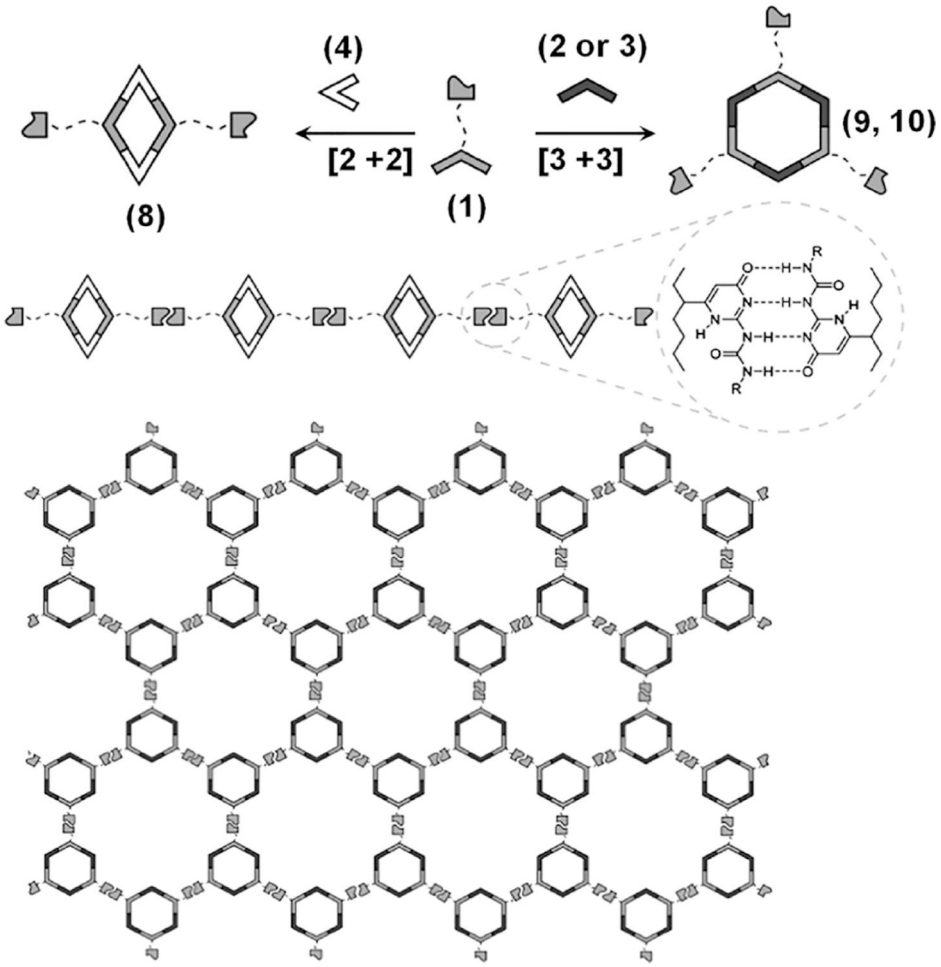

Figure 2.

Synthesis and supramolecular polymerization of UPy-functionalized rhomboid **8** and hexagons **9** and **10**. Adapted with permission from ref 14. Copyright 2013 National Academy of Sciences (USA).

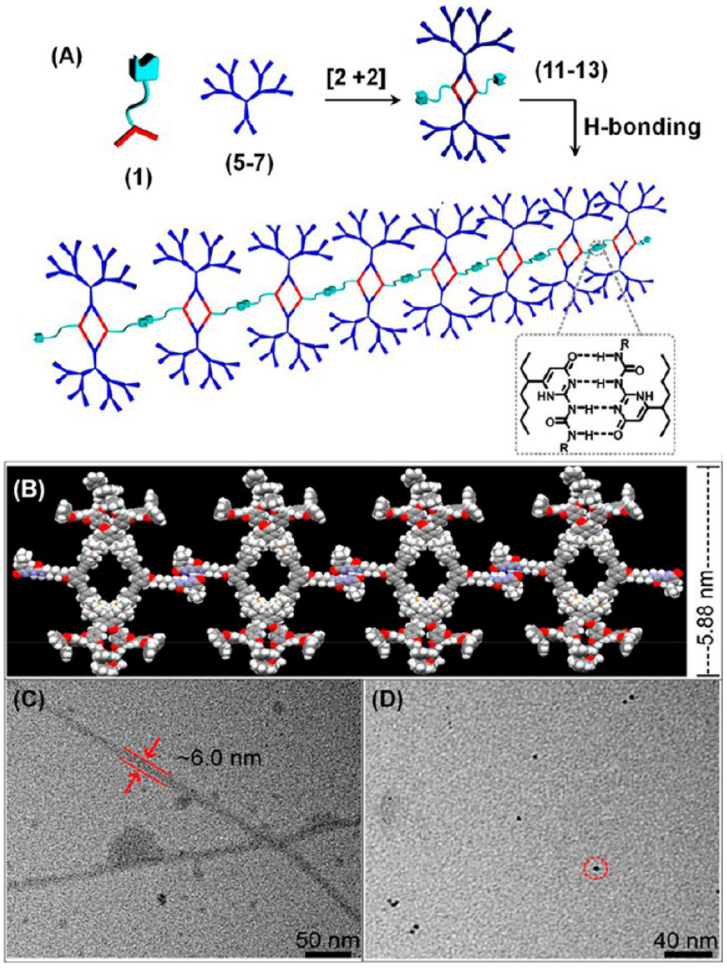

Figure 3.

(A) Synthesis and formation of DSPs of UPy-functionalized rhomboids **11–13**. (B) DSP of **13** by PM6 semiempirical molecular orbital methods. TEM images of aggregates of **13** obtained from (C) CH_2Cl_2 and (D) DMSO. Adapted with permission from ref 15. Copyright 2013 American Chemical Society.

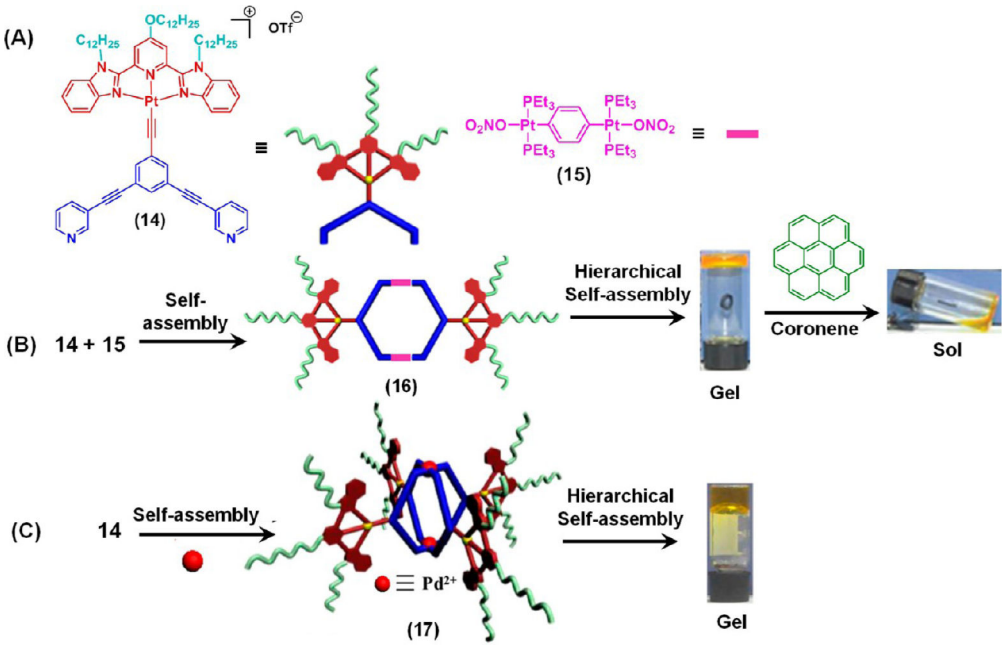

Figure 4.

HAS-mediated metallogelation by **16** and **17**. Stimuli-responsive behavior of the metallogel obtained from **16**. Panel B Adapted with permission from ref 16. Copyright 2016 Wiley-VCH; Panel C Adapted with permission from ref 17. Copyright 2018 American Chemical Society.

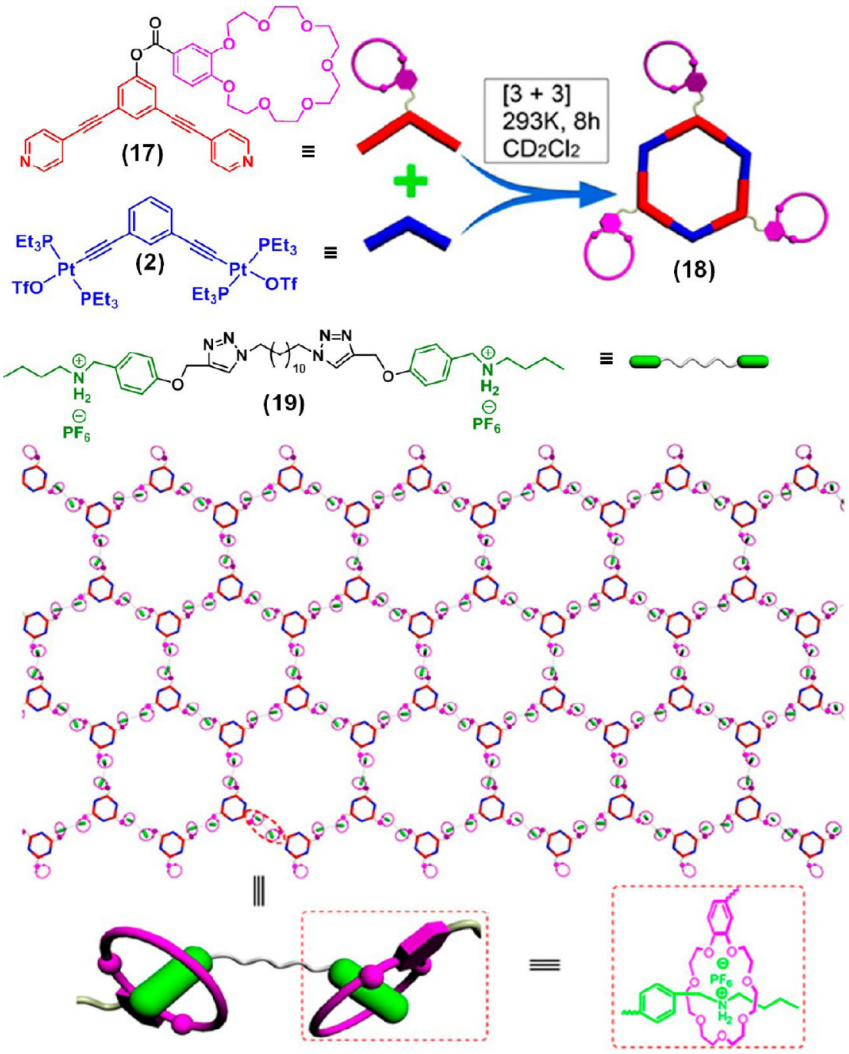

Figure 5.

Preparation of metallacycle **18** and its host–guest complexation with bisammonium salt **19** forming a supramolecular polymeric network. Adapted with permission from ref 18. Copyright 2014 American Chemical Society.

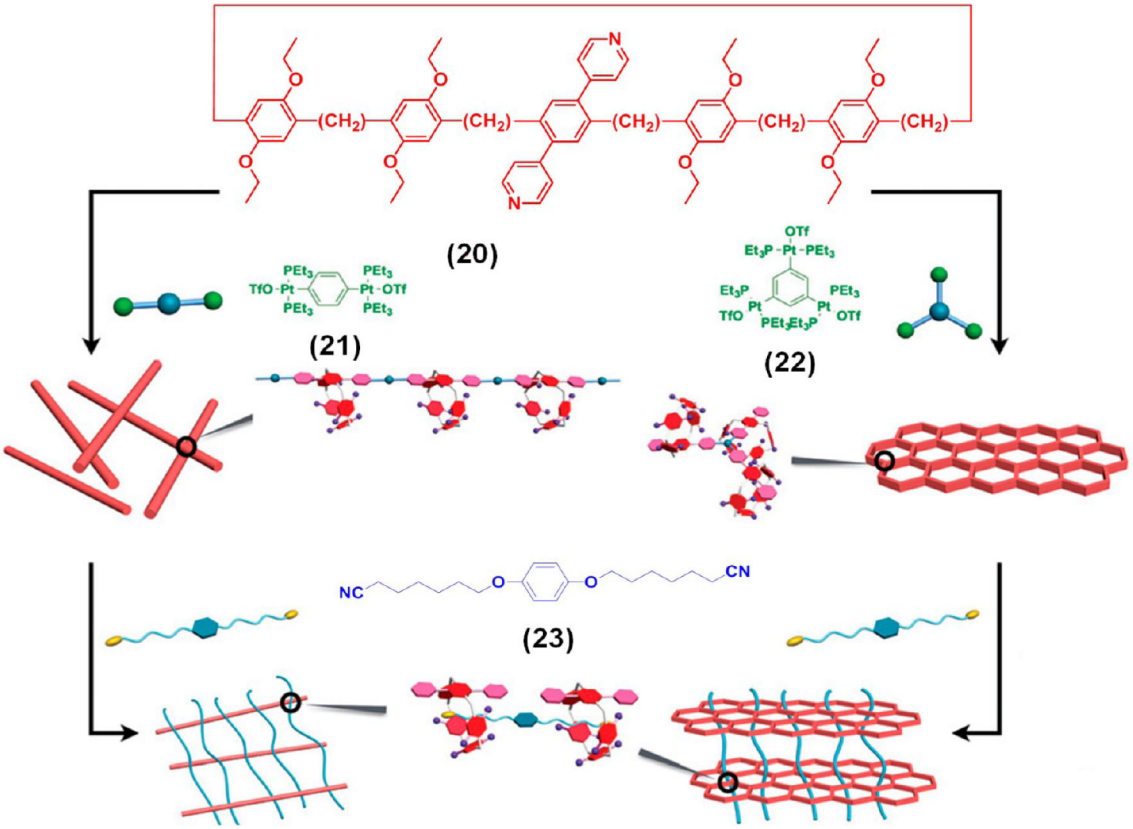

Figure 6.

Schematic illustration of supramolecular metallogelation via HAS of **20** with **21–23**. Adapted with permission from ref 21. Copyright 2017 The Royal Society of Chemistry.

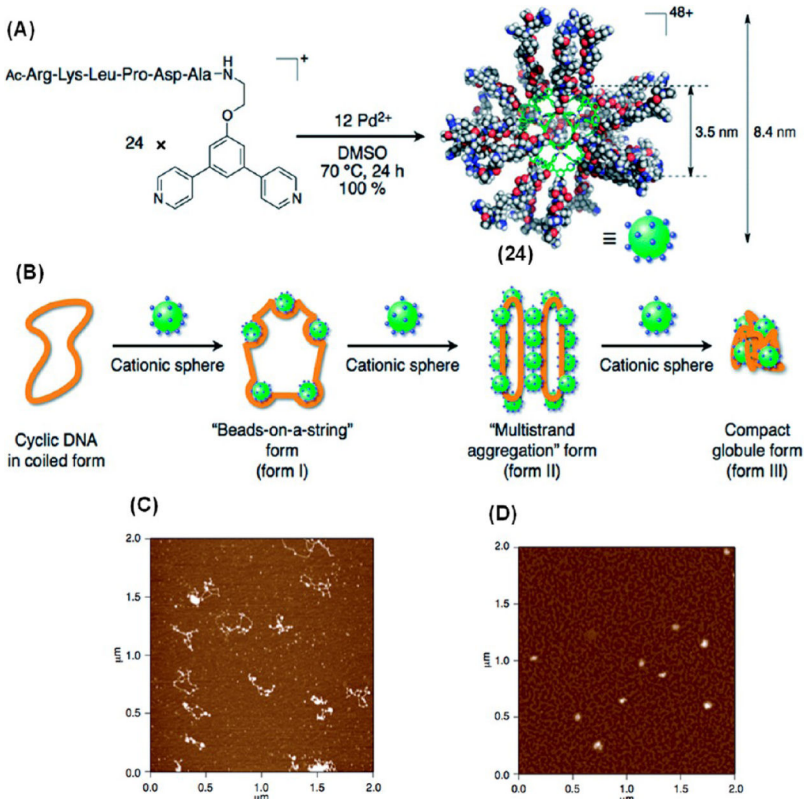

Figure 7.

(A) Preparation of **24**. (B) Schematic illustration and (C, D) AFM images of various morphologies obtained during DNA compaction by **24**. Adapted with permission from ref 25. Copyright 2014 The Royal Society of Chemistry.

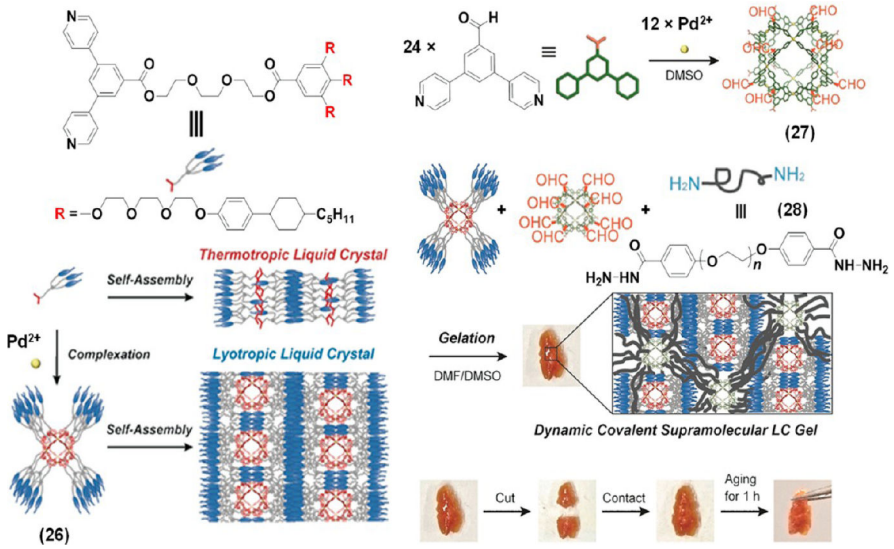

Figure 8.

Schematic illustration of the formation of a LC polymer gel from **26**. Adapted with permission from ref 28. Copyright 2017 Wiley-VCH.

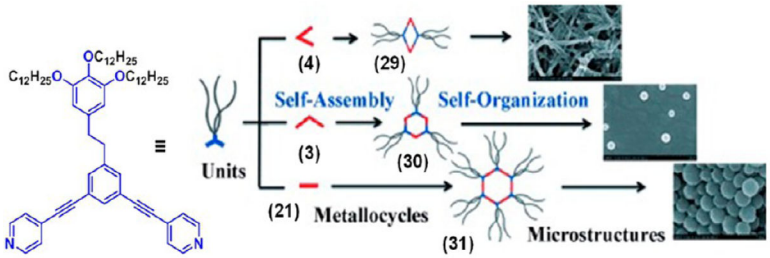

Figure 9.

Various nanostructures formed by compounds **29–31**. Adapted with permission from ref 29. Copyright 2014 Wiley-VCH.

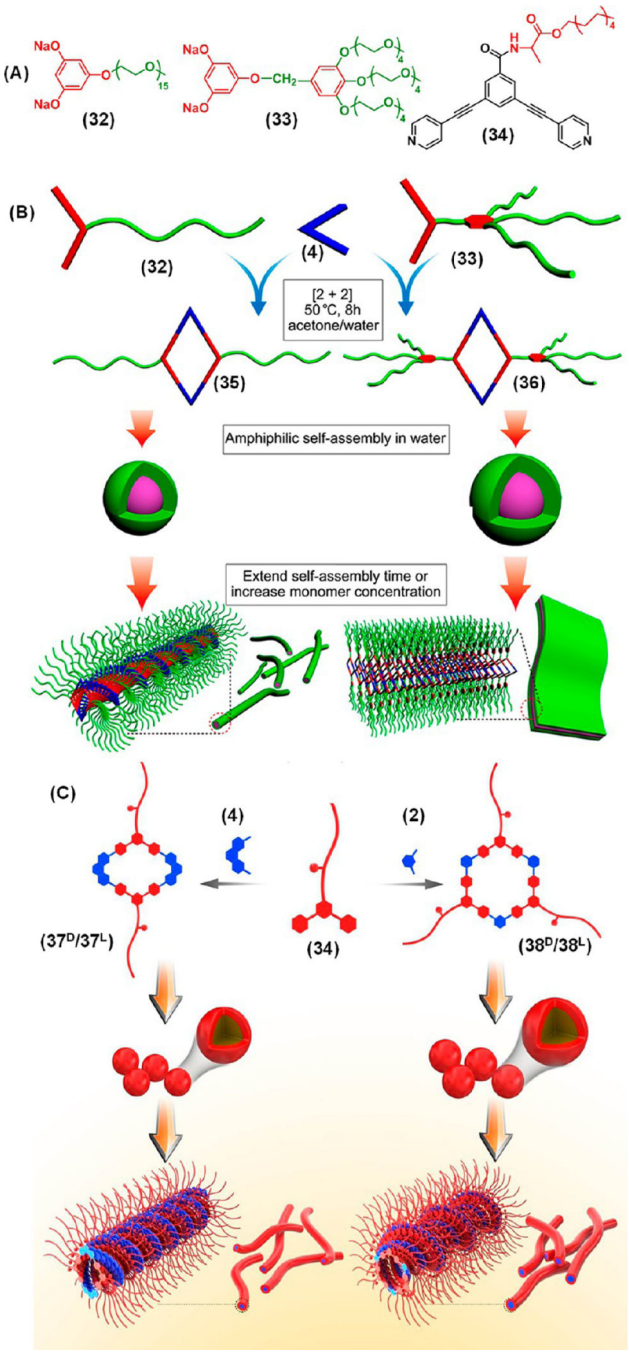

Figure 10.

(A) Precursors reported by Yan et al.[30] and Sun et al.[31] for the preparation of metallacycles. Schematic illustration of the formation of various nanostructures by (B) **35** and **36** and (C) $\mathbf{37^D/37^L}$ and $\mathbf{38^D/38^L}$ depending upon concentration. Panel B Adapted with permission from ref 30. Copyright 2013 American Chemical Society. Panel C Adapted with permission from ref 31. Copyright 2017 American Chemical Society.

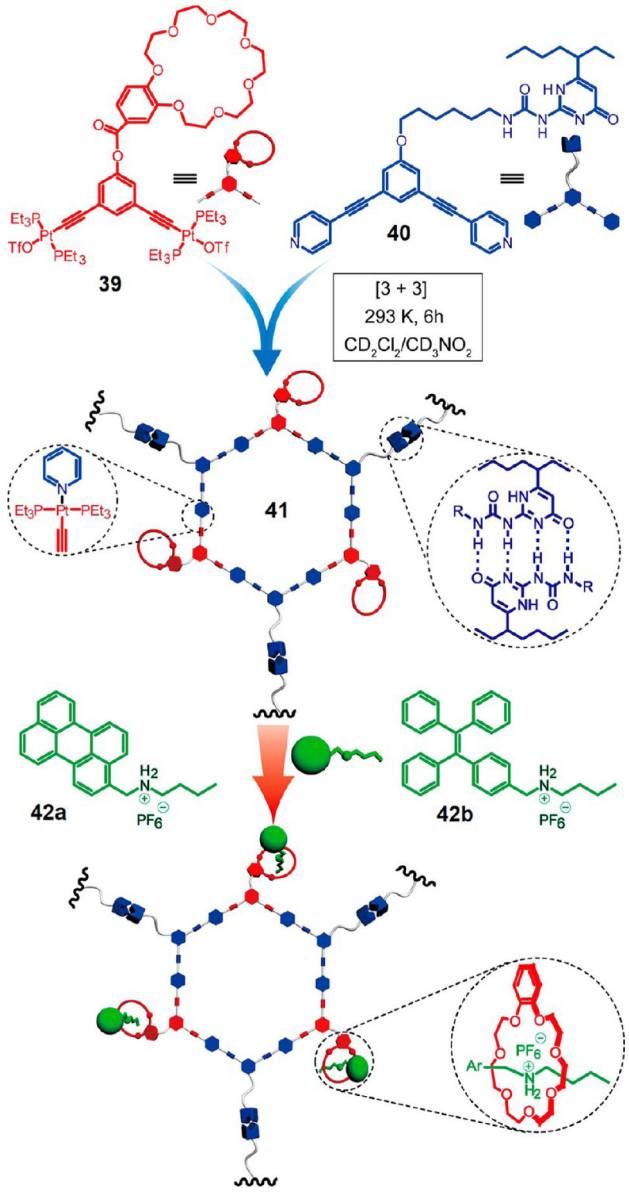

Figure 11.

HAS of **39, 40,** and **42** via triply orthogonal noncovalent interactions. Adapted with permission from ref 32. Copyright 2016 American Chemical Society.

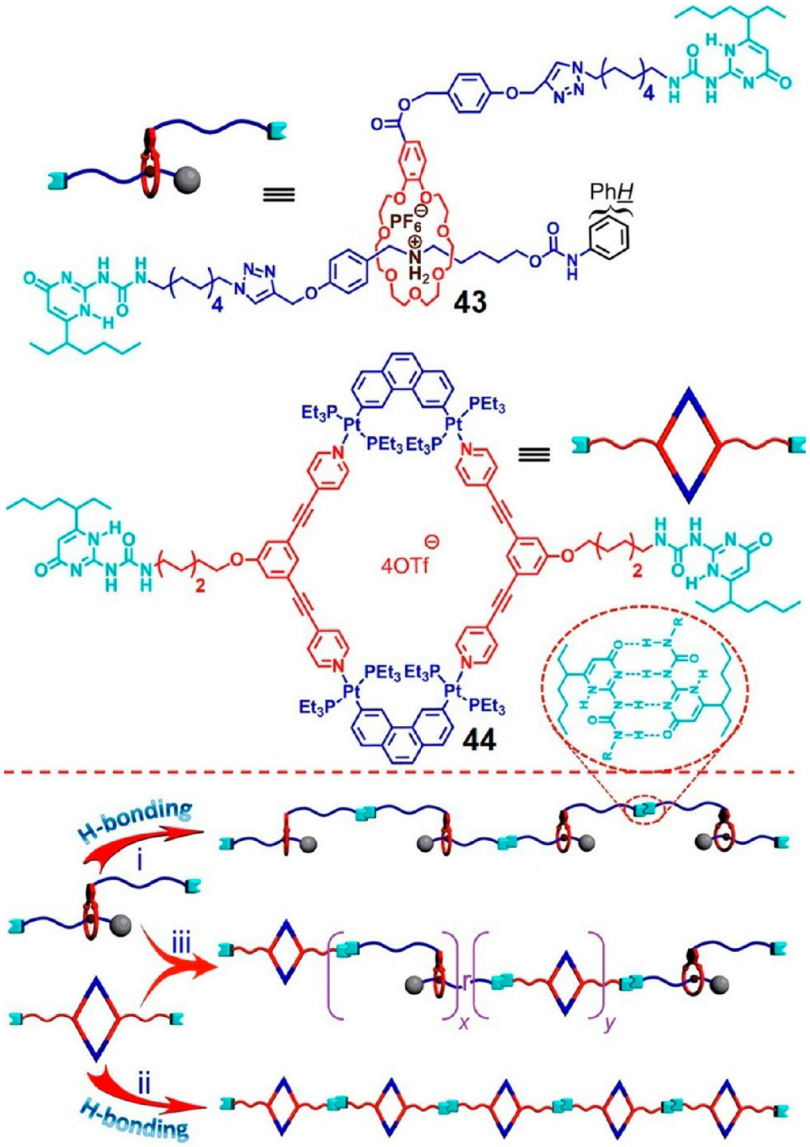

Figure 12.

Cartoon representations of formation of supramolecular copolymers by **43** and **44**. Adapted with permission from ref 33. Copyright 2016 American Chemical Society.

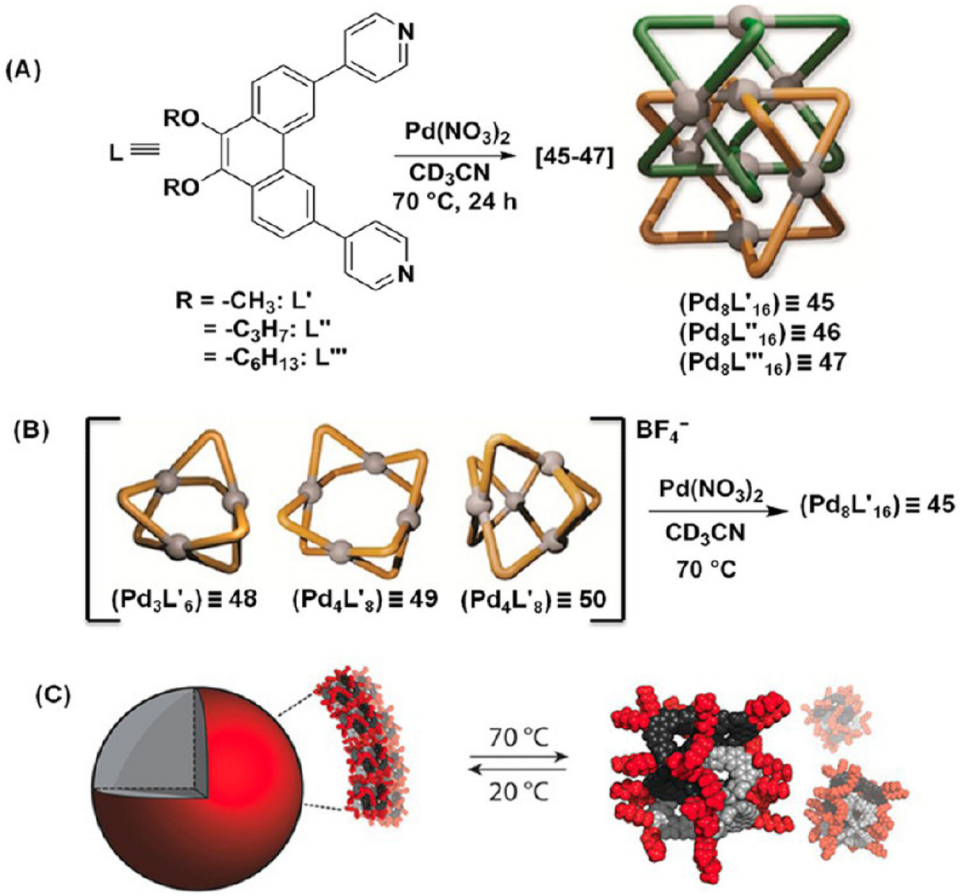

Figure 13.

(A) Preparation of [2]catenanes **45–47**. (B) The NO_3^- triggered transformation of **48–50** into **45**. (C) Thermoresponsive behavior of **47**. Adapted with permission from ref 35. Copyright 2018 Wiley-VCH Verlag GmbH & Co. KGaA, Weinheim.

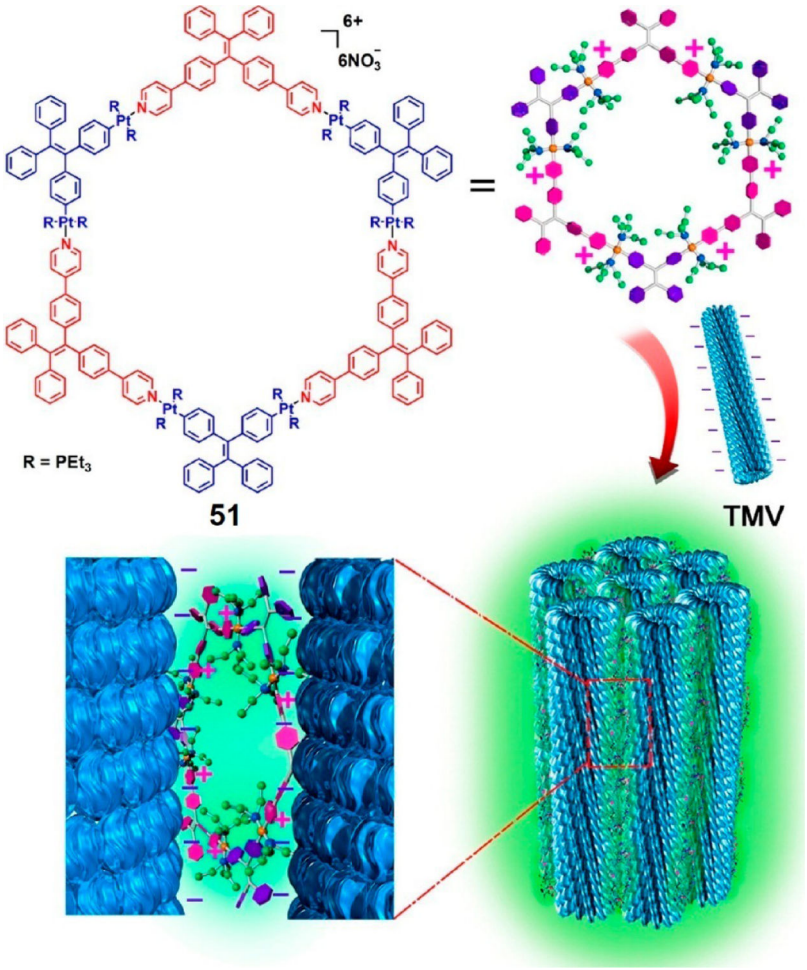

Figure 14.
Synthesis of **TMV/51** biohybrid. Adapted with permission from ref 37. Copyright 2016 American Chemical Society.

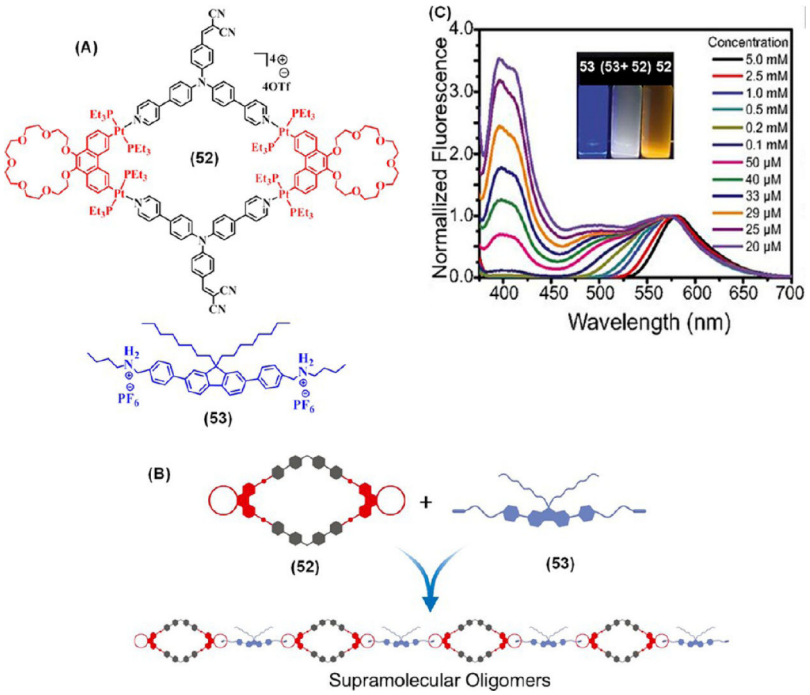

Figure 15.

(A) Molecular structures of **52** and **53** and (B) their supramolecular oligomerization. (C) Emission spectra of 1:1 mixture of **52** and **53** at different concentrations. Inset shows photographs of 52 (right), 53 (left), and mixture of equimolar **52** and **53** (middle) in acetone under 365 nm UV-light. Panels B and C Adapted with permission from ref 39. Copyright 2017 National Academy of Sciences (USA).

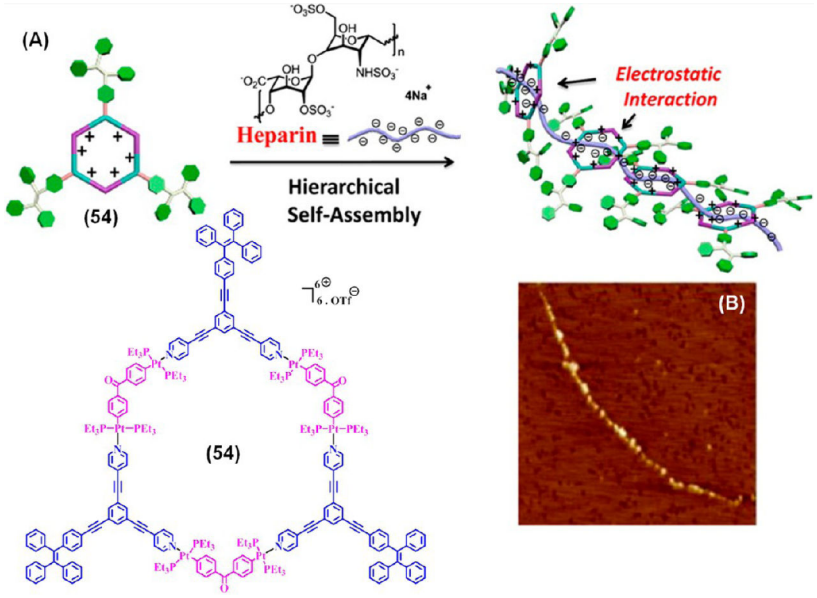

Figure 16.

(A) Schematic representation and (B) AFM image of the HAS of **54** and heparin. Adapted with permission from ref 41. Copyright 2015 American Chemical Society.

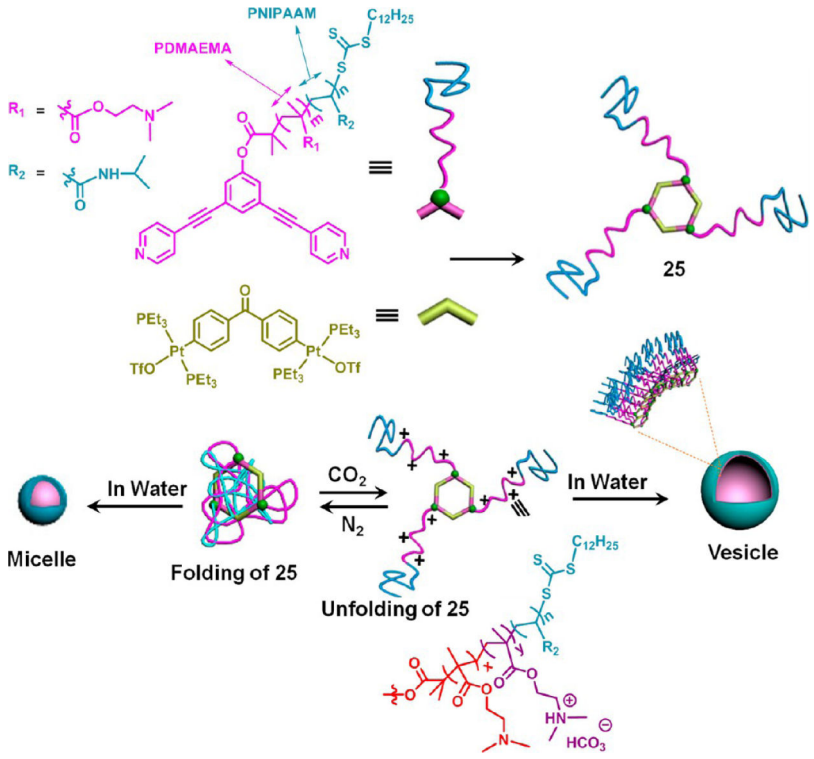

Figure 17.

CO_2-responsive morphological transformation of **25** in water. Adapted with permission from ref 42. Copyright 2017 American Chemical Society.

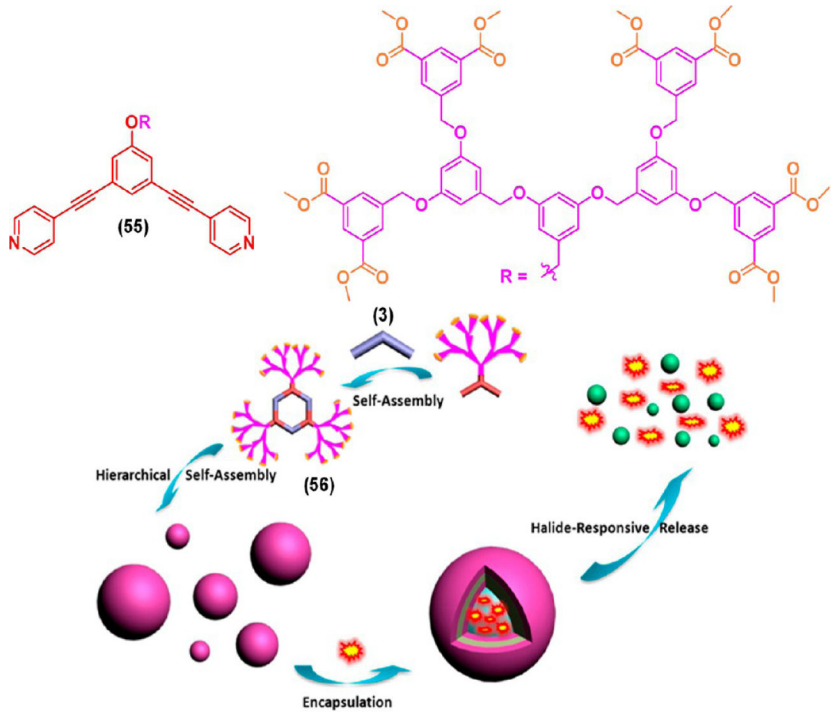

Figure 18.

Synthesis of a hexagonal metallodendrimer **56** from **3** and **55**, its HAS into vesicles and micelles, and the subsequent halide-induced controlled release of guests. Adapted with permission from ref 43. Copyright 2014 American Chemical Society.

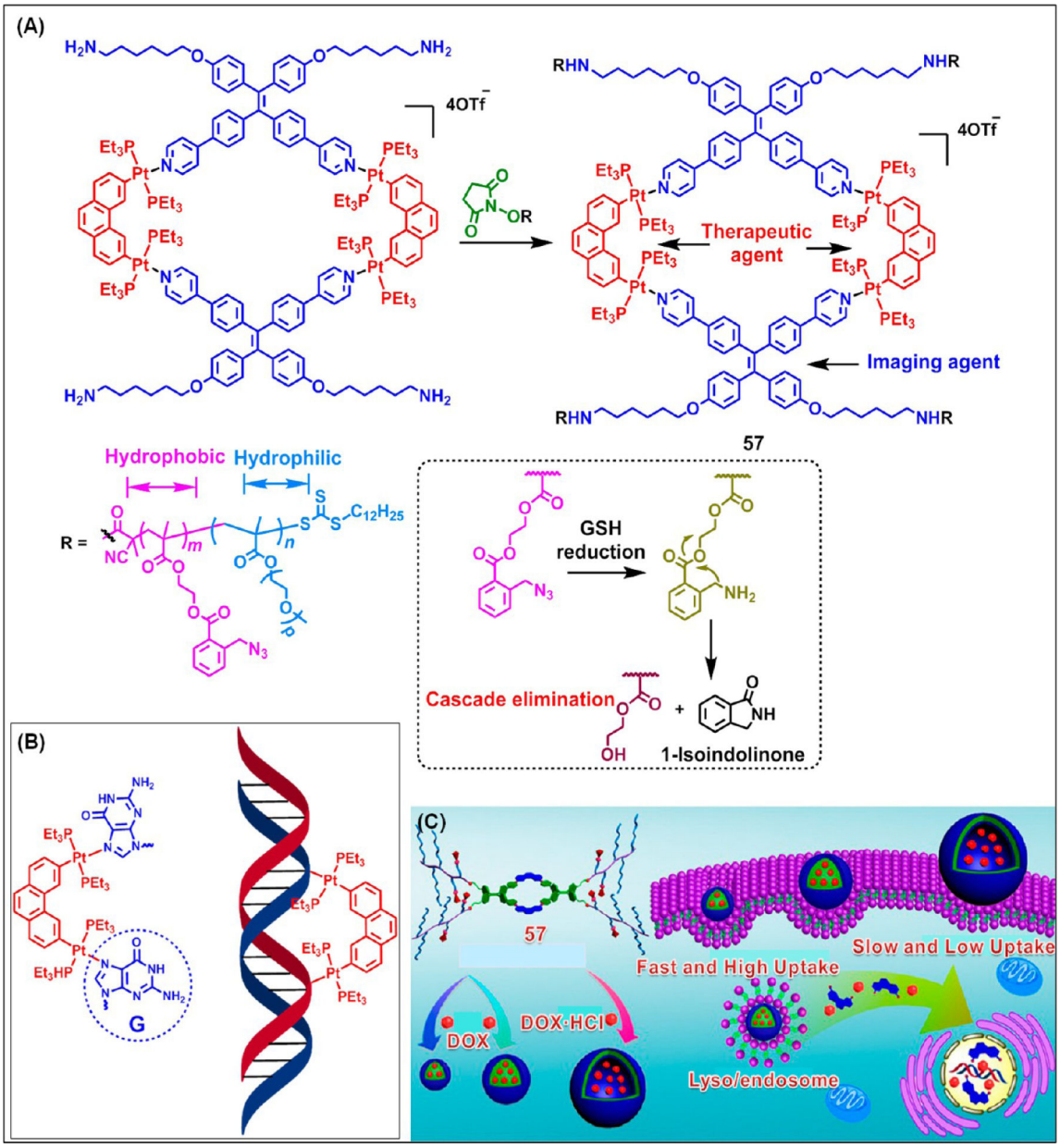

Figure 19.

(A) Synthesis and GSH-triggered cascade elimination reaction of **57**. (B) Cross-linking of **PhenPt** with DNA. (C) Schematic representation of the cellular uptake of DOX-loaded nanostructures self-assembled from **57**. Panel C adapted with permission from ref 44. Copyright 2017 American Chemical Society.

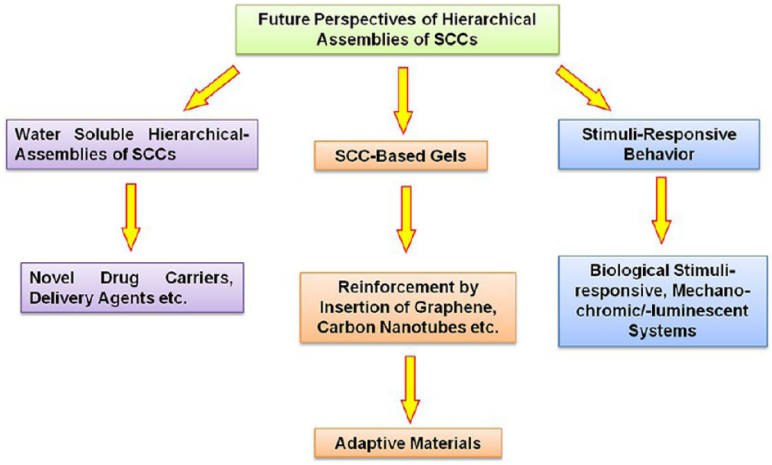

Figure 20.
Schematic illustration of promising future prospects of HASs of SCCs.

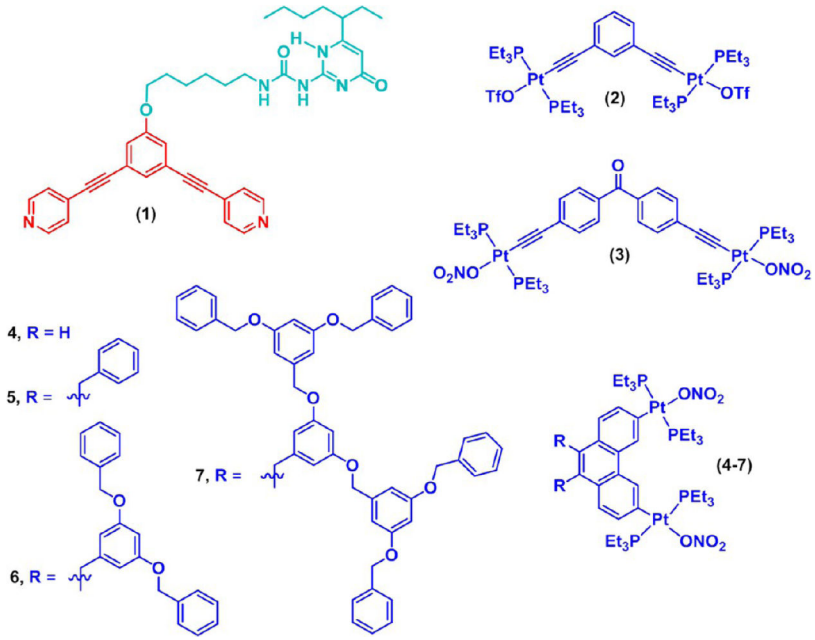

Chart 1.
Precursors 1–7 Reported by Yan et al.[14] for the Preparation of Metallacycles

Table 1.

Strength and Compatibility of Various Interactions Used in the SCC-based HASs

		HASs of SCCs via combination of orthogonal interactions			
strength of interactions	**type of interactions**[a]	**dual orthogonal interactions**	**morphologies**	**properties**	**refs**
weak (0–15 kcal/mol)	HI	MLC and HI	spheres, fibers, ribbons	gel	29–31
	π*–*π	MLC and ***π*–*π***	rods, fibers	gel	16, 17
	HB				
moderate (15–60 kcal/mol)	MHB	MLC and MHB	fibers	gel	14, 15
	MLC				
strong (>60 kcal/mol)	II	MLC and II	“beads-on-a-string”, globules	DNA condensation, AIE	25, 37, 41
	HGI	MLC and HGI	fibers	gel, white light emission	18–21
	DCB	MLC and DCB		self-healing gel	28

[a]HI = hydrophobic interactions; ***π*–*π*** = ***π*–*π*** stacking; HB = hydrogen bonding; MHB = multiple-hydrogen bonding: MLC = metal–ligand coordination; II = ionic interactions; HGI = host–guest interactions, DCB = dynamic covalent bonding.